

Absolute Polarization Determinations of 36 Pulsars Using the Green Bank Telescope

Megan M. Force,¹ Paul Demorest² & Joanna M. Rankin¹

¹*Physics Department, University of Vermont, Burlington, VT 05405**

²*National Radio Astronomy Observatory, Charlottesville, VA 22903*

Accepted 2011 month day. Received 2011 month day; in original form 2011 month day

ABSTRACT

Absolute polarimetry observations of 36 pulsars were carried out with the Green Bank Telescope in the 1100-1900-MHz band using the GUPPI backend. This group was selected to help complete a larger sample for which accurate proper-motion measurements were available. A combination of profile analysis using the core/double cone model and polarization-angle fitting methods were applied to estimate the “fiducial” longitude of the magnetic axis for each star and refer the linear polarization angle at that point to infinite frequency. As had been found previously, a number of the pulsars are found to have fiducial polarization directions that fall either along or at right angles to their proper-motion directions, whereas upwards of a third of the stars studied show alignments that are neither parallel or orthogonal.

Key words: – pulsars: general

1 INTRODUCTION

We report here on an absolute polarimetry study of 36 pulsars, observed with the Green Bank Telescope in West Virginia. This work amplifies the conclusion, first clearly articulated by Johnston *et al.* (2006; hereafter Johnston I) that many pulsars exhibit orderly alignments between their linear polarization and proper motion directions on the sky. Inspired by this work, a number of further alignments were assembled by Rankin (2007), observations of other pulsars were carried out by Johnston *et al.* (2007; hereafter Johnston II) and a reevaluation of the existing alignments was published by Noutsos *et al.* (2012).

Questions about pulsars’ large space velocities and the orientations of supernova “kicks” are much older than Johnston I. In an effort to explore these questions, major surveys of absolute linear polarimetry were pioneered by the Bonn group (Morris *et al.* 1979, 1981); however, these failed to show proper-motion alignments due both to the small sample then available and the poor quality of timing determinations. Strangely, Deshpande *et al.* suffered a similar difficulty as late as 1999.

Following widespread assumption that pulsars emitted by the curvature process, it seemed obvious that that orientation of the linearly polarized radiation must be **parallel** to the projected magnetic field direction. Even after the discovery that pulsars emit in two orthogonal

(hereafter OPM) polarization modes (Rankin *et al.* 1974; Manchester *et al.* 1975), many assumed that the “primary” polarization mode must be parallel. This easy presumption was dashed in the new millennium by X-ray imaging of the Vela pulsar (Helfand *et al.* 2001; Radhakrishnan & Deshpande 2001) where arcs indicated the orientation of the star’s rotation axis Ω relative to its polarization and proper-motion (hereafter PM) directions. Shockingly, the radiation was polarized orthogonally to the magnetic field B plane, a circumstance then beautifully confirmed for the radio emission by Johnston I.

For most pulsars, of course, the direction of the rotation axis Ω on the sky must be deduced from the electric vector orientation of its radiation at a rotational phase thought to represent the magnetic axis longitude. At this “fiducial” instant, a pulsar’s beam faces the Earth squarely and the projected magnetic field associated with its emission is \parallel to Ω . Thus the “fiducial” polarization position angle (hereafter PPA) PA_0 is measured and referred to infinite frequency as a proxy for the (unseen) orientation of the rotation axis Ω . Values for PA_0 can then be compared with well determined proper-motion (hereafter PM) directions PA_v , defining the orientation angle $\Psi = PA_v - PA_0$.

In the following sections, then, we present absolute, infinite-frequency polarization profiles for the observed pulsars. These were studied and classified in terms of the system described in Rankin (1993a,b) in order to better understand the emission geometry and the relationship of

* meganforce@hotmail.com; Joanna.Rankin@uvm.edu

Table 1. Observational parameters.

Pulsar	MJD	Resolution (msec)	Length (secs)
B0011+47	55729.762	0.606	1832
B0136+57	55729.787	0.133	1217
B0149-16	55752.399	0.407	1506
B0320+39	55729.805	1.480	2437
B0458+46	55729.837	0.312	1825
B0656+14	55729.863	0.188	1832
B0906-17	55729.888	0.196	1785
B1039-19	55751.860	0.677	1670
B1112+50	55729.916	0.809	1832
B1237+25	55751.894	0.675	1211
B1322+83	55729.941	0.327	3058
B1325-43	55751.942	0.260	1732
B1508+55	55729.980	0.361	1739
B1540-06	55751.919	0.346	1645
B1703-40	55752.178	0.284	1800
B1718-02	55751.967	0.233	1217
B1718-32	55752.121	0.233	1825
B1732-07	55751.985	0.205	1632
B1757-24	55752.146	0.061	2440
B1800-21	55752.203	0.065	1227
B1821-19	55752.220	0.092	1258
B1826-17	55752.238	0.150	1518
B1838-04	55752.260	0.091	1500
B1839+56	55753.317	0.807	1832
B1905+39	55753.342	0.604	2034
B1911-04	55752.281	0.403	1525
B1929+10	55752.110	0.111	605
B1929+10	55753.397	0.111	605
B2106+44	55753.408	0.203	1825
B2111+46	55753.433	0.496	1825
B2148+63	55729.631	0.186	2231
B2154+40	55729.661	0.745	1525
B2217+47	55729.682	0.263	1529
B2224+65	55729.703	0.333	2372
B2255+58	55729.733	0.180	959
B2310+42	55729.748	0.170	916
B2319+60	55752.310	1.102	1217
B2324+60	55752.328	0.114	1620
B2327-20	55752.376	0.803	1645
B2351+61	55752.350	0.461	1620

the polarization traverses to the fiducial longitude. Wherever possible the PPA traverse was fitted using the single-vector model (Radhakrishnan & Cooke 1969; hereafter SVM) and referred to infinite frequency using an accurate rotation measure (hereafter RM) stemming from our observation. In §2 we discuss our observations, and in §3 the profile analyses conducted to determine the fiducial longitudes. §4 presents the fiducial PPA analyses, and §5 a summary and discussion of the results.

2 OBSERVATIONS

The observations were carried out in the summer of 2011 using the 100-m Robert C. Byrd Green Bank Telescope (hereafter GBT) and the GUPPI pulsar backend in coherent filterbank mode. The dates and lengths of the var-

[H]

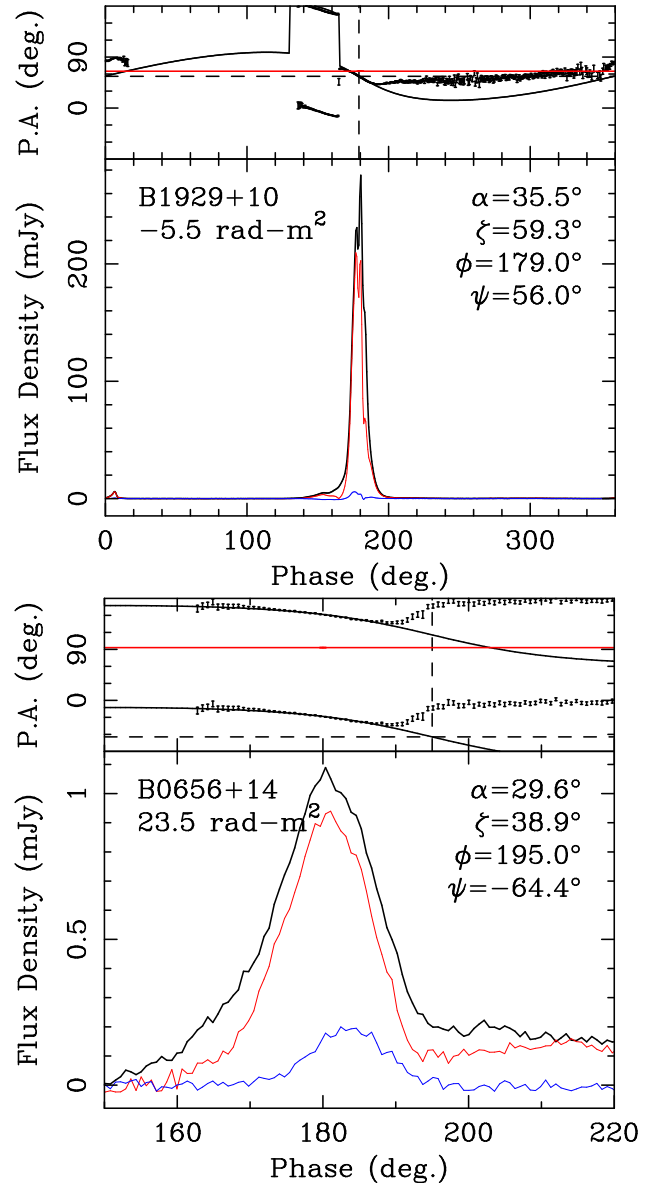


Figure 1. Polarization profiles and absolute PPA information for pulsars B1929+10 and B0656+14, which served as primary calibrators for the observation project. The lower panels give the total power (Stokes I ; heavy black curve), total linear polarization (Stokes L ; red curve) and total circular polarization (Stokes V ; blue curve). The upper panels give the measured polarization position-angle (hereafter PPA) values—derotated to infinite frequency according to the specified RM—with their errors as well as a fitted curve computed using the rotating-vector model (hereafter RVM). The pulsar proper-motion direction on the sky is indicated by a red horizontal line (blue when shifted by 180° .) The pulsar names are given at the upper left and the fitted parameter values at the upper right of the lower panels.

Table 2. Proper-motions directions, absolute fiducial PPAs, and orientation angles for 36 pulsars

PSR	PA_v (deg)	PA_0 (deg)	Ψ (deg)
B0011+47	+136(3)	+43(7)	-87(8)
B0136+57	-131(0)	+43(3)	+6(3)
B0149-16	+173(2)	-86(15)	+80(15)
B0320+39	+158(8)	-39(2)	+17(9)
B0458+46	-45(19)	-9(2)	-36(20)
B0656+14	+93(0)	-65(7)	-21(7)
B0906-17	+167(2)	-27(14)	+14(14)
B1039-19	-4(12)	-12(1)	+8(12)
B1112+50	+157(2)	-35(2)	+11(2)
B1237+25	-65(0)	-20(1)	-45(1)
B1322+83	-76(14)	+26(3)	+78(15)
B1325-43	+3(5)	-4(7)	+7(9)
B1508+55	-130(0)	-7(2)	+56(2)
B1540-06	-103(10)	+66(2)	+10(10)
B1703-40	+5(35)	+5(1)	0(35)
B1718-02	-178(9)	-8(10)	+10(13)
B1718-32	-179(7)	-62(1)	+63(7)
B1732-07	-5(3)	-22(1)	+17(4)
B1757-24	+146(137)	-65(2)	+32(137)
B1800-21	+3(5)	+15(1)	-12(5)
B1821-19	-173(17)	+53(2)	-46(17)
B1826-17	+172(9)	+11(1)	-19(9)
B1838-04	+11(40)	—	—
B1839+56	-125(5)	+56(2)	-1(5)
B1905+39	+45(10)	+66(1)	-21(10)
B1911-04	+166(6)	-20(1)	+6(6)
B1929+10	+65(0)	+52(1)	+13(1)
B1929+10	+65(0)	+56(0)	+9(1)
B2106+44	+68(26)	+69(7)	-1(27)
B2111+46*	-20(44)	-86(0)	+66(44)
B2148+63	+54(12)	-58(20)	-67(23)
B2154+40	+76(0)	+83(7)	-7(7)
B2217+47	-158(10)	+65(4)	-44(11)
B2224+65m	+52(1)	-48(5)	+100(5)
B2255+58	+106(12)	+24(3)	+82(12)
B2310+42	+76(0)	+18(0)	+58(0)
B2319+60	—	-60(0)	—
B2324+60*	-60(24)	+49(1)	+72(24)
B2327-20	+86(2)	+28(2)	+59(3)
B2351+61	+75(9)	+48(1)	+27(9)

* Hobbs *et al.* give the PMs for these two pulsars in ecliptic coordinates. The respective coordinate systems are offset from each other by a rotation angle of $3.5^\circ \cos RA \cos Dec$ which for both stars is 12° . As they both lie in the vicinity of the vernal equinox, the rotations ccw from North are positive.

ious observations are given in Table 1. Full-Stokes spectra were acquired in an 800-MHz bandwidth centered at 1500 MHz radio frequency; the ~ 1200 – 1300 MHz airport radar analog filter was used, resulting in a ~ 700 -MHz effective bandwidth. The filterbank frequency resolution was 1.5 MHz, or 512 channels across the full band. The data were coherently dedispersed in real time using the

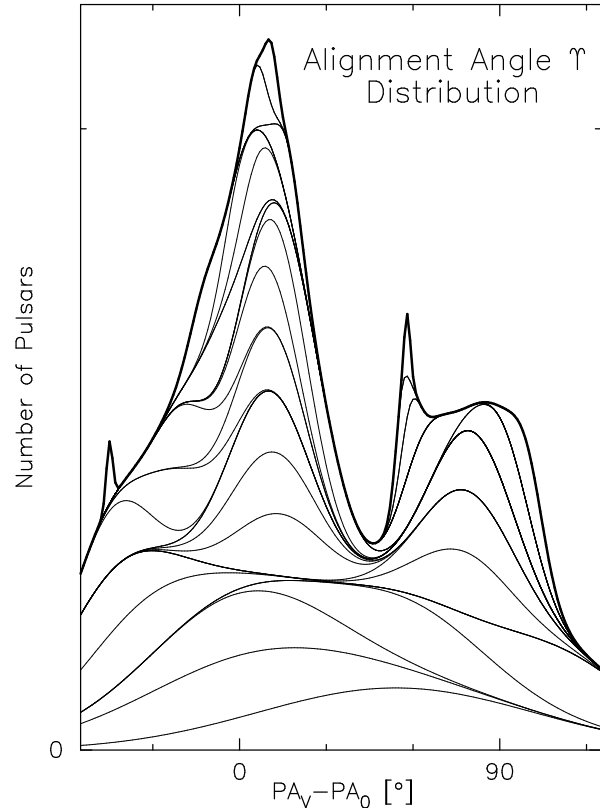


Figure 2. Distribution of alignment angles $\Psi [= PA_v - PA_0]$. Values are given for 34 pulsars represented by Gaussians centered on the value and with widths reflecting the estimated error. No useful values were available for either B1757-24 or B2319+60, nor were redundant values developed for the calibrators B0656+14 and B1929+10.

catalogued¹ dispersion measure for each pulsar to remove in-channel dispersive smearing, then integrated in time for 20 μ s per spectrum and recorded to disk. The filterbank data were then “folded” modulo the current apparent pulse period into the final full-Stokes pulse profiles. In all cases the final profile resolution was $1/2048$ of the pulsar’s rotation period (hereafter P_1) and these resolutions are also given in Table 1. The filterbank files were then inspected for radiofrequency interference (hereafter RFI) and the corrupted areas masked out in frequency and time.

Flux and polarization calibration were performed using the PSRCHIVE software package (Hotan *et al.* 2004). Paired with each pulsar, an observation of a locally-generated standard noise source was recorded to determine the flux scale. The equivalent noise source flux density was determined during our project via observation of the unpolarized quasar J1445+0958, with an assumed flux at 1500 MHz of 2.32 Jy. From a 3-hour observation of the pulsar B0450+55, taken as part of a different observing program using an identical instrumental setup, the rotation of the source with respect to the telescope was

¹ ATNF pulsar catalogue (Manchester *et al.* 2005); <http://www.atnf.csiro.au/research/pulsar/psrcat>

used to solve for the receiver system’s intrinsic polarization cross-coupling matrix, following van Straten (2004). From the calibrated profiles versus frequency, we determined rotation measures (RM) using the PSRCHIVE program “rmfit” as follows: We first determined an initial RM by finding the RM value that maximized the total linearly polarized flux in the frequency-averaged profile. After applying the initial RM, the full band was averaged into upper and lower halves, and the weighted mean position angle difference between the two halves was used to find the final RM and its uncertainty (*e.g.* Han et al 2006). RM determinations for all sources are tabulated in Table A2. Note that while for the purposes of PPA determination we used the directly measured RM, to facilitate comparison with other work we have applied a correction for the expected ionospheric contribution to the values presented in Table A2. The calibrated profiles were then RM de-rotated, corrected for parallactic angle, and integrated over the full band—thus providing the basis for the analyses described in the following sections.

3 POLARIZATION PROFILE ANALYSIS

Absolute fiducial PPA determinations require accurate measurements of three different types: a) absolute polarimetry (PPAs measured CCW from North on the sky) at the frequency of observation; b) rotation-measure values to refer the PPAs to infinite frequency; and c) profile analyses to estimate the “fiducial” longitude of a pulsar’s magnetic axis.

Our three-fold analyses to these ends are largely presented in the Appendix below. The results of the observational calibrations and reductions from the GBT are given in Figures A1–A9 below. Each figure gives the results for four pulsars. The total power, linear and circular polarization of the profile are given in the lower panels, while the PPA information is given in the upper ones. Here the PPAs have been referred to infinite frequency, and a horizontal curve showing the proper-motion direction PA_v is also indicated (red, or blue if shifted by 180°).

Two different approaches were used to estimate the fiducial longitude and thus the fiducial PPA PA_0 . First, we reassessed the totality of the available published polarized profile information on the 36 pulsars in an effort to determine the nature of their sightline traverses using the core/double cone model of ET VI and the other papers of this series. The results of these efforts are discussed in paragraphs on each star in the Appendix and summarized in Table A2. In addition, we fitted single-vector model curves to the PPA traverses of each pulsar wherever possible. The longitude origins of each profile in Figs A1–A9 show the inflection points of these curves, and the resulting parameters are given on each plot. In some cases, of course, it was necessary to correct for orthogonal polarization mode “jumps”, and these are indicated as relevant. Low level polarized RFI was present in some of the observations, and in some cases seems to have affected our RM measurements and RVM fits. Therefore in a few cases we manually restricted the pulse longitude range used for the RM and/or RVM fits to avoid data we believe to be corrupted. In some cases we have even ar-

gued for a different fiducial longitude than that given by the fitting. These issues are discussed in detail for each pulsar in the Appendix.

4 PROPER-MOTION & FIDUCIAL PPA ANALYSIS

Three pulsars with well measured fiducial polarization angles were included in our observations as calibrators, and several other such stars were included in order to better understand their fiducial geometry. Panels showing the absolute polarization and proper-motion orientations for pulsars B0656+14 and B1929+10 are given as Figure 1 (B1237+25 appears in Fig. A3 below). For none of the three is it straightforward to directly compare their fiducial polarization directions, as in the former two cases they are offset from the star’s profile peak and in the latter this point falls at an exceedingly steep point on the PPA traverse. Moreover, low level polarized RFI appears to distort the PPA traverses of both stars in Fig. 1 near the fiducial longitude. So, rather, we have used the PPA values at the profile peaks to compare our observations with published ones. Not surprisingly, the strongest correspondence is for B1929+10, where our $+54^\circ$ PPA at the profile peak could be squared with that of Johnston I within a degree or two. Our B0656+14 profile also has a peak PPA that corresponds to that in Rankin (2007) with an uncertainty of 5° , as does our B1237+25 fiducial PA_0 correspond to that of Johnston I within about the same margin. Finally, our PA_0 for B1911–04 is identical to that of Johnston I but with an uncertainty of 8° .

5 SUMMARY AND DISCUSSION

The relationship between the proper-motion direction PA_v and the fiducial polarization angle direction PA_0 are given in Table 2 for the 36 pulsars under study. These values reflect the analyses discussed above as well as the specific circumstances of each pulsar as discussed in the Appendix.

As shown in Figure 2 the alignment values appear to fall into three rough groups. About half of the stars show alignments such that their fiducial polarization directions are parallel to their proper-motion directions within a few degrees. A few others appear to have orthogonal alignments, and the remaining third show intermediate alignments such as were determined accurately earlier for pulsars B1237+25 and B1508+55.

Along with Johnston I, II, Rankin (2007) and Noutsos *et al.* (2008) this effort brings the number of pulsars with well studied fiducial polarization alignments to over 100. Or to say it differently, fiducial polarimetry investigations have now been carried out for most of the non-millisecond pulsar population having accurately determined proper motions. The parallel or perpendicular alignments reflect uncertainties in both the emission direction relative to the projected magnetic field direction and questions about whether supernovae impart natal “kicks” parallel or perpendicular to their rotation direction. In addition, some older pulsars may misalign from

their natal orientation due to Galactic acceleration and other causes. Finally, it must be remembered that proper motions provide only two of the components of a pulsar's velocity, and in general no means exist to determine the third. Therefore, for some pulsars that lie in particular directions relative to the Earth and the Galactic plane, lack of this third velocity component results in an incomplete and distorted picture of a pulsar's Ω orientation relative to its PA_v direction.

In light then of OPM uncertainties, the relative orientation of pulsar rotation and velocity vectors remains unknown. However, evidence from the increasingly large sample of pulsars for which this analysis has been performed lends plausibility to the asymmetrical "kick" theory for the origins of observed high space velocities in these stars. A high velocity "kick", delivered during the collapse of a pulsars stellar progenitor, remains the most accepted explanation for these velocities in the current understanding. A second 90° ambiguity is also present in neutron-star birth theories which suggest that vectors would be orthogonal or aligned depending on the length of the natal "kick" delivered by the supernova explosion (Spruit and Phinney 1998). Broad peaks centered at 0° and 90° , such as seen in Fig 2, suggest a trend toward parallel or perpendicular vectors, while misalignment often appears to correspond to greater characteristic pulsar spin down ages.

6 ACKNOWLEDGMENTS

The authors wish to thank Dr. Aris Noutsos for his advice and assistance with the analyses and Joel Weisberg for providing ionospheric rotation-measure estimates. Portions of this work were carried out with support from US National Science Foundation Grants AST 08-07691. The Green Bank Telescope is operated by the National Radio Astronomy Observatory under contract to the US National Science Foundation. This work used the NASA ADS system.

REFERENCES

- Briskin, W. F., Benson, J. M., Goss, W. M., & Thorsett, S. E. 2002, *Ap.J.*, 571, 906
- Briskin, W. F., Fruchter, A. S., Goss, W. M., Herrnstein, R. M., & Thorsett, S. E. 2003, *A.J.*, 126, 3090
- Chatterjee, S., Cordes, J. M., Vlemmings, W.H.T., Arzoumanian, Z., Goss, W. M., & Lazio, T.J.W. 2004 *Ap.J.*, 604, 339
- Chatterjee, S., Briskin, W. F., Vlemmings, W.H.T., Goss, W. M., Lazio, T.J.W., Cordes, J. M., & Thorsett, S. E. 2009, *Ap.J.*, 698, 250
- Deshpande, A. A., Ramachandran, R., & Radhakrishnan, V. 1999, *A&A*, 351, 195
- Everett, J. E., & Weisberg, J. M. 2001, *Ap.J.*, 553, 341
- Hamilton, P. A., & Lyne, A. G. 1987, *MNRAS*, 224, 1073
- Han, J. L., Manchester, R. N., & Qiao, G. J. 1999, *MNRAS*, 306, 371
- Han, J. L., Manchester, R. N., Lyne, A. G., Qiao, G. J., & van Straten 2006, *Ap.J.*, 642, 868
- Helfand, D. J., Gotthelf, E. V., & Halpern, J. P. 2001, *Ap.J.*, 556, 380
- Hotan, A. W., van Straten, W., & Manchester, R. N. 2004, *PASA*, 21, 302
- Johnston, S., Hobbs, G., Vigeland, S., Kramer, M., Weisberg, J. M., & Lyne, A. G. 2006, *MNRAS*, 364, 1397 (Johnston I)
- Johnston, S., Kramer, M., Karastergiou, A., Hobbs, G., Ord, S., & Wallman, J. 2007, *MNRAS*, 381, 1625 (Johnston II)
- Manchester, R.N. 1972, *Ap.J.*, 172, 43.
- Manchester, R.N. 1974, *Ap.J.*, 188, 637.
- Manchester, R.N., Taylor, J.H., & Huguenin, G.R. 1975, *Ap.J.*, 196, 83.
- Manchester, R. N., Hobbs, G. B., Teoh, A., & Hobbs, M. 2005, *A.J.*, 129, 1993
- Morris, D., Graham, D. A., Sieber, W., Jones, B. B., Seiradakis, J. H., & Thomasson, P. 1979, *A&A*, 73, 46
- Morris, D., Graham, D. A., Sieber, W., Bartel, N., & Thomasson, P. 1981, *A&A Suppl.*, 46, 421 (MGSBT)
- Ng, C.-Y., & Romani, R. W., 2004, *Ap.J.*, 601, 484
- Noutsos, A., Johnston, S., Kramer, & Karastergiou, A. 2008, *MNRAS*, 386, 1881
- Noutsos, A., Kramer, M., Carr, P., & 2012, *MNRAS*, 423, 2736
- Qiao, G. J., Manchester, R. N., Lyne, A. G., & Gould, D. M. 1995, *MNRAS*, 274, 572
- Radhakrishnan, V., & Cooke, D. J. 1969, *Ap. Lett.*, 3, 225
- Radhakrishnan, V. & Deshpande, A. A. 2001, *A&A*, 379, 551
- Rand, R. J., & Lyne, A. G. 1994, *MNRAS*, 268, 497
- Rankin, J. M. 1993a, *Ap.J.*, 405, 285 (ET VIa)
- Rankin, J. M. 1993b, *Ap.J. Suppl.*, 85, 145 (ET VIb)
- Rankin, J. M. 2007, *Ap.J.*, 664, 443
- Spruit, H. & Phinney, E. S. 1998, *Nature*, 393 (6681), 139.
- Rankin, J. M., Campbell, D. B., & Backer, D. C. 1974, *Ap.J.*, 188, 609
- van Straten, W. 2004, *Ap.J. Suppl.*, 152, 129
- Taylor, J. H., Manchester, R. N., & Lyne, A. G. 1993, *Ap.J. Suppl.*, 88, 529
- Thorsett, S., Briskin, W. F., & Goss, W. M. 2002, *Ap.J.*, 573, L111
- Weisberg, J. M., Cordes, J. M., Kuan, B., Devine, K. E., Green, J. T., & Backer, D. C. 2004, *Ap.J. Suppl.*, 150, 317
- Zou, W. Z., Hobbs, G., Wang, N., Manchester, R. N., Wu, X. J., & Wang, H. X. 2005, *MNRAS*, 362, 1189

APPENDIX A: CLASSIFICATION AND GEOMETRY

In order to appropriately interpret the polarization position-angle (hereafter PPA) traverses of the various pulsars, we consulted the body of available published polarimetry, the profile classifications in ET VI (Rankin 1993) and occasionally the fluctuation spectra of Weltevrede *et al.* (2006, 2007; hereafter WES/WSE).

B0011+47: Little is known about this star. Our profile together in Figure A1 with those of GL suggest a triple **T** profile with a weak trailing “outrider”, and the WES/WSE fluctuation spectra provide weak support for this interpretation. R is -5.7° both in Table A1 and the fitted RVM curve in the above figure. This said, the fit is poor, and it makes no sense for the PPA inflection point to fall as late as it does. We take the fiducial longitude to fall at the peak of the profile at 181° where the PPA is $+43^\circ$.

B0136+57 seems to be reliably classified as having an S_t profile on the basis of weak conal “outriders” visible in the 1.7-5 GHz band. The nominal geometry in ET VI using the core-width information then provides a basis for the PPA fitting in Fig. A1. This fitting, however, seems misleading as the inflection point falls far too late to be reliable. We therefore took the fiducial longitude to be near the center of the central (putative core) component at a longitude of 181.5° , where the PPA is $+43^\circ$.

B0149–16 was supposed to have a triple **T** profile in ET VI, but our profile in Fig. A1 together mainly with those of GL suggest an evolution more like that of an inner cone double **D** profile—and a drift feature is reported by WES/WSE. The small fractional linear polarization makes the PPA difficult to track, but both the large early rotation and the OPM dominance shift later are seen in other published profiles (*e.g.* GL at 408 MHz). LM’s R value of about 30° is born out by the values in the RVM fit. The fiducial longitude is fixed at 184.3° .

B0320+39: The evidence is strong and consistent that this 3-sec pulsar has a conal single S_d profile as shown in Fig. A1. The low frequency profiles exhibit pronounced bifurcation, and a strong drift feature is seen by Izvekova *et al.* (1982) and by WES/WSE. The RVM fit suggests a much steeper PPA traverse than was envisioned in ET VI. The PPA rotation on the leading edge seems unreliable because of the depolarization there. We have thus fitted to the flat part of the traverse and assumed an unresolved 180° rotation at around the linear polarization minimum near 183° longitude.

B0458+46: ET VI interpreted this profile as **T**, and vH’s 4.9-GHz profile appears to seal the case. WES/WSE report a flat fluctuation spectrum. Nonetheless, the very small L/I makes the PPA difficult to fit and interpret reliably in Figure A2. Apparently the PPA slope is positive, but our fitted R value is very different than that in ET VI.

B0906–17 may have a triple **T** profile. The Johnston I profile at 21 cm, those of GL, and vH’s 4.9-GHz profile suggest this structure most clearly. WES/WSE again report a flat fluctuation spectrum. Nonetheless the low L/I and prominent OPM dominance shift on the leading edge make the PPA difficult to fit, and indeed Johnston I found

no satisfactory fit. Several profiles suggest A/R and our fit in Fig. A2 strongly verifies its presence. The RVM fit and Table A1 geometries are comparable in terms of the β values.

B1039–19 exhibits a classic double conal (**M** or **cQ**) profile along with the nearly 180° , ‘S’-shaped PPA traverse—and WES/WSE report clear evidence of modulation. This behavior is very well exhibited in the work of Mitra & Li (2004) and provides a secure basis for RVM fitting and interpretation in Fig. A2. Both the α and β values compare closely in Table A1 and the above figure.

B1112+50: ET VI classed this star as having an S_t profile, and indeed its core does seem to fall out of the center of its profile at 21 cms. and above. WES/WSE, however, detect drifting in the first component and Wright *et al.* (1986) moding and nulling. Overall, little PPA rotation can be seen across the profile in Fig. A2. The β values compare closely in Table A1 and the above figure. No RVM fit, however, suffices to fix the fiducial longitude, so we have fixed it near the core peak at 180.3° longitude where the PPA is -35° .

B1237+25 is the classic pulsar with a five-component profile, and its three modes were studied in detail by Stroslik & Rankin (2005) and recently by Smith *et al.* (2013), where its highly steep PPA traverse is exhibited in its quiet normal mode. The pulsar was also among those whose absolute PPA alignment was determined in Johnston I. It was included here in Figure A3 as a diagnostic of the polarimetry and PPA fitting.

B1322+83 has a strange very wide “double” profile which ET IX (see their fig. A3, lower left) interpreted as consisting of a precursor and a trailing single profile. WSE find that the star has a flat fluctuation spectrum, thus the best guess is that the trailing feature is a S_t profile. Moreover, the PPA traverse is flat under the precursor and linear under the trailing feature, so we have no recourse but to assume that the fiducial longitude coincides with the profile midpoint; see Fig. A3.

B1325–43: We find only two published profiles for this pulsar, those of WMLQ and MHQ, and these give no clear picture regarding the star’s evolution. Fortunately, the PPA traverse in Fig. A3 is well defined, so the fitted fiducial point seems fully reliable.

B1508+55: Absolute PPA measurement were first conducted for this pulsar by Morris *et al.* (1979, 1981), and it appears to represent a highly interesting case of misalignment as documented by Chatterjee *et al.* (2005). We included the pulsar as a diagnostic. Its triple **T** profile is well studied and modeled in ET VI as a foundation for the fitting in Fig. A3. The RVM fit inflection, however, appears to fall a bit late; if we take the fiducial longitude at the profile peak, as did Morris *et al.*, we get a fiducial PPA of -6.5° and an alignment angle of $+56^\circ$, not far from their $+45(4)^\circ$.

B1540–06: ET VI correctly classed this pulsar as having a conal single S_d profile, and indeed the strong drift features identified by WES/WSE confirm the classification definitively. The polarization is slight, but the central PPA traverse agrees with that of GL, perhaps indicating an unresolved OPM dominance transition. The linear polarization in the far wings of the profile in Figure A4 is probably due to RFI.

Table A1. Emission-Beam Geometry of the Sample Pulsars

PSR	Class	α	$ \Delta\chi/\Delta\varphi _o$ ($^\circ/^\circ$)	β	$\Delta\Psi$	Inner ρ	β/ρ	$\Delta\Psi$	Outer ρ	β/ρ	r Inner	(km) Outer
B0011+47	T?	10	-5.7	-1.7	45	3.9	-0.44	—	—	—	128	—
B0136+57	St	44	+5.3 ^a	+7.5	~10	8.6	0.87	—	—	—	135	—
B0149-16	D?	84	+30 ^a	+1.9	8.2	4.5	0.42	—	—	—	113	—
B0320+39	Sd	69	+23	+2.3	—	—	—	~5	3.3	0.70	—	221
B0458+46	T?	14	+2.2	+6.4	—	—	—	~20	7.0	0.91	—	211
B0906-17	arT	31	-6?	4.9	17?	6.8	0.73	—	—	—	124	—
B1039-19	M	31	-18 ^a	+1.7	~13	3.8	0.43	17	4.8	0.34	136	214
B1112+50	St?	30	+10.1	2.8	7	3.4	0.84	—	—	—	126	—
B1237+25	M	53	-149	-0.3	8.6	3.5	-0.09	12.3	4.9	0.06	110	220
B1322+83m	St?	14	+2.8	5.1	12?	5.4	0.95	—	—	—	130	—
B1325-43	St?	—	—	—	—	—	—	—	—	—	—	—
B1508+55	T	45	-15	-2.7	11	4.7	-0.58	—	—	—	109	—
B1540-06	Sd	59	-14?	3.5	9?	5.3	0.67	—	—	—	131	—
B1703-40	?	—	—	—	—	—	—	—	—	—	—	—
B1718-02	Sd?	23	-12	-1.9	—	—	—	43	8.2	-0.23	—	214
B1718-32	D?	30	∞	0.0	24?	6.0	0.0	—	—	—	114	—
B1732-07	T?	54	∞	0.0	17	6.8	0.0	—	—	—	131	—
B1757-24	?	—	—	—	—	—	—	—	—	—	—	—
B1800-21	St?	16	-1.8	-8.8	88	11.9	0.74	—	—	—	126	—
B1821-19	St?	70	-36	-1.5	—	—	—	—	—	—	—	—
B1826-17	T?	39	+50 ^a	+0.7	~24	7.7	0.09	—	—	—	120	—
B1839+56	T	38	∞	0.0	~11	3.4	0.0	—	—	—	126	—
B1905+39	M	33	-15 ^a	2.1	~12	4.0	0.53	16.4	5.1	0.41	131	214
B1911-04	St	64	-27 ^a	-1.9	9.8	4.8	-0.40	—	—	—	125	—
B2106+44	D?	38	∞	0.0	~22	6.8	0.0	—	—	—	127	—
B2111+46	T	9	-6.7 ^a	1.4	—	—	—	66	5.8	0.24	—	229
B2148+63	Sd	10.5	+1.5 ^a	7.0	13.9	7.2	0.97	—	—	—	130	—
B2154+40	cT?	21	+8*	+2.6	—	—	—	20.1	4.6	0.56	—	214
B2217+47	St	42	+8.5	4.5	12.0	6.1	.73	—	—	—	135	—
B2224+65m	St?	27	-3.6	4.9	—	—	—	—	—	—	—	—
B2255+58	St	24	—	—	—	—	—	—	—	—	—	—
B2310+42	M?	56	+7	+6.8	9.7	8.0	0.85	~15	9.4	0.73	148	204
B2319+60	cQ?	18	-8 ^a	+2.2	~10	2.8	0.80	19	3.9	0.58	117	225
B2324+60	St?	62	6?	+8.5	~7	9.0	0.94	—	—	—	127	—
B2327-20	T	66	+43	1.2	7.0	3.4	0.35	—	—	—	128	—
B2351+61	?	65	-12	-4.3	—	—	—	~9	5.9	-0.73	—	219

B1703-40: Fig. A4 Little else is known about this pulsar with a strongly scattered profile even at 21 cms. The PPA traverse is expectedly flat, so we have not recourse but to take the fiducial longitude at the profile peak. The RVM fit, of course, is meaningless.

B1718-02 shows a conal single \mathbf{S}_d evolution, asymmetric single profile near 21 cms. and an unresolved component pair at meter wavelengths; see GL . WSE/WSE further see drift features confirming the classification. The PPA traverse in Fig. A4, however, is so nearly linear that it poorly fixes the fiducial longitude. A better estimate comes from taking the PPA value at the profile center near 185° longitude where the fiducial PPA is -8° .

B1718-32: Little is known about this pulsar, the available profiles (GL, WMLQ) add little to ours in Fig. A4, and no fluctuation-spectrum seems to exist. The PPA traverse is well developed and RVM-like, but the fit is quite poor in terms of χ_2 as is clear from the plot.

B1732-07: The evidence seems strong that this pulsar's profile is dominated by a central core component sur-

rounded by one or two pairs of conal “outriders”—this it is either of the \mathbf{M} or \mathbf{T} class. By far the best published profiles are those in Johnston II, though GL and vH are worth inspection. In this context, the PPA traverse strongly resembles that on B1237+25 and thus represents an unresolved steep 180° S'-shaped RVM function. The fiducial PPA must then be 90° away from the flat leading and trailing sections in Figure A5.

B1757-24: Little is known about this pulsar, but GL do confirm the shallow negative-going PPA traverse. The far edge emission in Fig. A5 and large acceleration potential make \mathbf{S}_t the best guess. Fortunately, the large fractional linear polarization gives a reliable PPA fit.

B1800-21: This star's unusual profile has attracted considerable attention, most notable vH's comparative study that includes GL's work. One might take this as an unusual conal double \mathbf{D} profile, but what appears to be a weak core is visible both in our Fig. A5 and GL's 1.41-GHz profile, and the star's acceleration potential is enormous; thus, the appropriate classification is \mathbf{T} triple or

Table A2. Proper motions, rotation measures and absolute polarization angles for 36 pulsars

PSR Bname	PSR Jname	Period P_1 (sec)	Age $\log(\tau)$ (yrs)	Proper Motion PA_v (deg)	Ref.	Rotation Measure Previous (rad m ⁻²)	Ref.	Measured (rad m ⁻²)	Fiducial PA_0 (deg)	Fig.
B0011+47	J0014+4746	1.241	7.54	+136(3)	1	—	—	-8.7(11)	+43(7)	A1
B0136+57	J0139+5814	0.272	5.61	-131(0)	2	-90(4)	1	-93.2(4)	+43(3)	A1
B0149-16	J0152-1637	0.833	7.01	+173(2)	1	+2(1)	2	+6.6(50)	-86(15)	A1
B0320+39	J0323+3944	3.032	7.88	+158(8)	3	+58(3)	1	+56.3(10)	-39(2)	A1
B0458+46	J0502+4654	0.639	6.26	-45(19)	3	-48(6)	1	-175.2(10)	-9(2)	A2
B0656+14	J0659+1414	0.385	5.05	+93(0)	4	+23.5(4)	3	—	-65(7)	1
B0906-17	J0908-1739	0.402	6.98	+167(2)	3	-36(6)	4	-32.1(7)	-27(14)	A2
B1039-19	J1041-1942	1.386	7.37	-4(12)	1	-16(5)	1	-22.8(5)	-12(1)	A2
B1112+50	J1115+5030	1.656	7.02	+157(2)	3	+3.2(5)	5	-0.1(8)	-35(2)	A2
B1237+25	J1239+2453	1.382	7.36	-65(0)	5	-0.3(1)	6	+3.9(3)	-20(1)	A3
B1322+83	J1321+8323	0.670	7.27	-76(14)	3	—	—	-23.2(11)	+26(3)	A3
B1325-43	J1328-6038	0.533	6.45	+3(5)	1	-41(3)	7	-22.9(9)	-4(7)	A3
B1508+55	J1509+5531	0.740	6.37	-130(0)	2	+0.8(7)	8	+3.1(4)	-7(2)	A3
B1540-06	J1543-0620	0.709	7.11	-103(10)	1	+4(4)	1	-1.8(8)	+66(2)	A4
B1703-40	J1707-4053	0.581	6.68	+5(35)	6	-207(25)	9	-179.7(5)	+5(1)	A4
B1718-02	J1720-0212	0.478	7.96	-178(9)	1	+17(3)	1	+6.0(15)	-8(10)	A4
B1718-32	J1722-3207	0.477	7.07	-179(7)	6	+90(7)	1	+70.4(5)	-62(1)	A4
B1732-07	J1735-0724	0.419	6.74	-5(3)	1	+8(3)	1	+34.5(3)	-22(1)	A5
B1757-24	J1801-2451	0.125	4.19	+146(137)	7	+637(12)	10	+605.7(5)	-65(2)	A5
B1800-21	J1803-2137	0.134	4.20	+3(5)	6	-27(3)	11	-36.1(2)	+15(1)	A5
B1821-19	J1824+1945	0.189	5.76	-173(17)	1	-303(15)	1	-302.2(7)	+53(2)	A5
B1826-17	J1829-1751	0.307	5.94	+172(9)	6	+306(6)	7	+304.7(4)	+11(1)	A6
B1838-04				+11(40)	8	+406(4)	11	—		
B1839+56	J1840+5640	1.653	7.24	-125(5)	3	-3(3)	1	-5.0(7)	+56(2)	A6
B1905+39	J1907+4002	1.236	7.56	+45(10)	3	+7(3)	1	+5.2(3)	+66(1)	A6
B1911-04	J1913-0440	0.826	6.51	+166(6)	3	+12(3)	4	+4.6(4)	-20(1)	A6
B1929+10	J1932+1059	0.227	6.46	+65(0)	9	-6.87(2)	4	-5.8(2)	+52(1)	1
B1929+10	J1932+1059	0.227	6.46	+65(0)	9	-6.87(2)	4	-5.5(2)	+56(0)	
B2106+44	J2108+4441	0.415	7.88	+68(26)	1	-146(9)	1	-433.0(6)	+69(7)	A7
B2111+46	J2113+4644	1.015	7.35	-20(44)	10	-224(2)	8	-218.8(1)	-86(0)	A7
B2148+63	J2149+6329	0.380	7.55	+54(12)	3	-160(7)	1	-156.5(3)	-58(20)	A7
B2154+40	J2157+4017	1.525	6.85	+76(0)	2	-44(2)	5	-32.6(30)	+83(7)	A7
B2217+47	J2219+4754	0.538	6.49	-158(10)	11	-35.3(18)	8	—	+65(4)	A8
B2224+65m	J2225+6535	0.683	6.05	+52(1)	3	-21(3)	1	—	-48(5)	A8
B2255+58	J2257+5909	0.368	6.00	+106(12)	6	-322(11)	1	-323.5(4)	+24(3)	A8
B2310+42	J2313+4253	0.349	7.69	+76(0)	2	+7(2)	1	+4.4(1)	+18(0)	A8
B2319+60	J2321+6024	2.256	6.71	—	—	-230(10)	1	-232.6(2)	-60(0)	A9
B2324+60	J2326+6113	0.234	7.02	-60(24)	10	-221(10)	1	-220.7(3)	+49(1)	A9
B2327-20	J2330-2005	1.644	6.75	+86(2)	1	+16(3)	1	+9.3(8)	+28(2)	A9
B2351+61	J2354+6115	0.945	5.96	+75(9)	3	-77(6)	1	-75.9(4)	+48(1)	A9

Proper motion references: (1) Brisken *et al.* (2003); (2) Chatterjee *et al.* (2009); (3) Harrison *et al.* (1993); (4) Ng & Romani (2004); (5) Brisken *et al.* (2002); (6) Zou *et al.* (2005); (7) Thorsett *et al.* (2002); (8) Johnston *et al.* (2007); (9) Chatterjee *et al.* (2004); (10) Hobbs *et al.* (2004); (11) Lyne *et al.* (1982) Rotation measure references: (1) Hamilton & Lyne (1987); (2) Qiao *et al.* (1995); (3) Weisberg *et al.* (2004); (4) Johnston *et al.* (2005); (5) Manchester (1974); (6) Taylor *et al.* (1993); (7) Han *et al.* (1999); (8) Manchester (1972); (9) Noutsos *et al.* (2008); (10) Han *et al.* (2006); (11) Rand & Lyne (1994)

perhaps a sort of M. WES report a flat fluctuation spectrum. Fortunately, the large fractional linear polarization prompts successful fitting for the fiducial longitude.

B1821-19: Little is known about this pulsar. Most of the GL profiles are poor and show little linear polarization. Fortunately, their 21 cm. profile is their best and largely agrees with our own in Fig. A5. WES/WSE report a flat fluctuation spectrum. The L form and large PPA rotation under the pulse suggests a core single \mathbf{S}_t profile with weak “outriders, providing a good foundation for fitting and interpretation of the PPA fiducial center.

B1826-17: This star has a triple profile per ET VI, and the supporting evidence (*e.g.* GL and MHQ) seems quite strong and consistent, as well as the flat fluctuation spectrum reported by WES. Remarkably, the PPA traverse in Figure A6 is completely flat once OPM dominance changes are accounted for—apart from the B1237+25-like 180° rotation at the profile center.

B1839+56 shows a clear \mathbf{T} triple structure at 102 MHz (MIS) but at all higher frequencies the three components appear to be conflated into an unresolved mass (GL). Moreover, only at 234 MHz does the PPA traverse seem

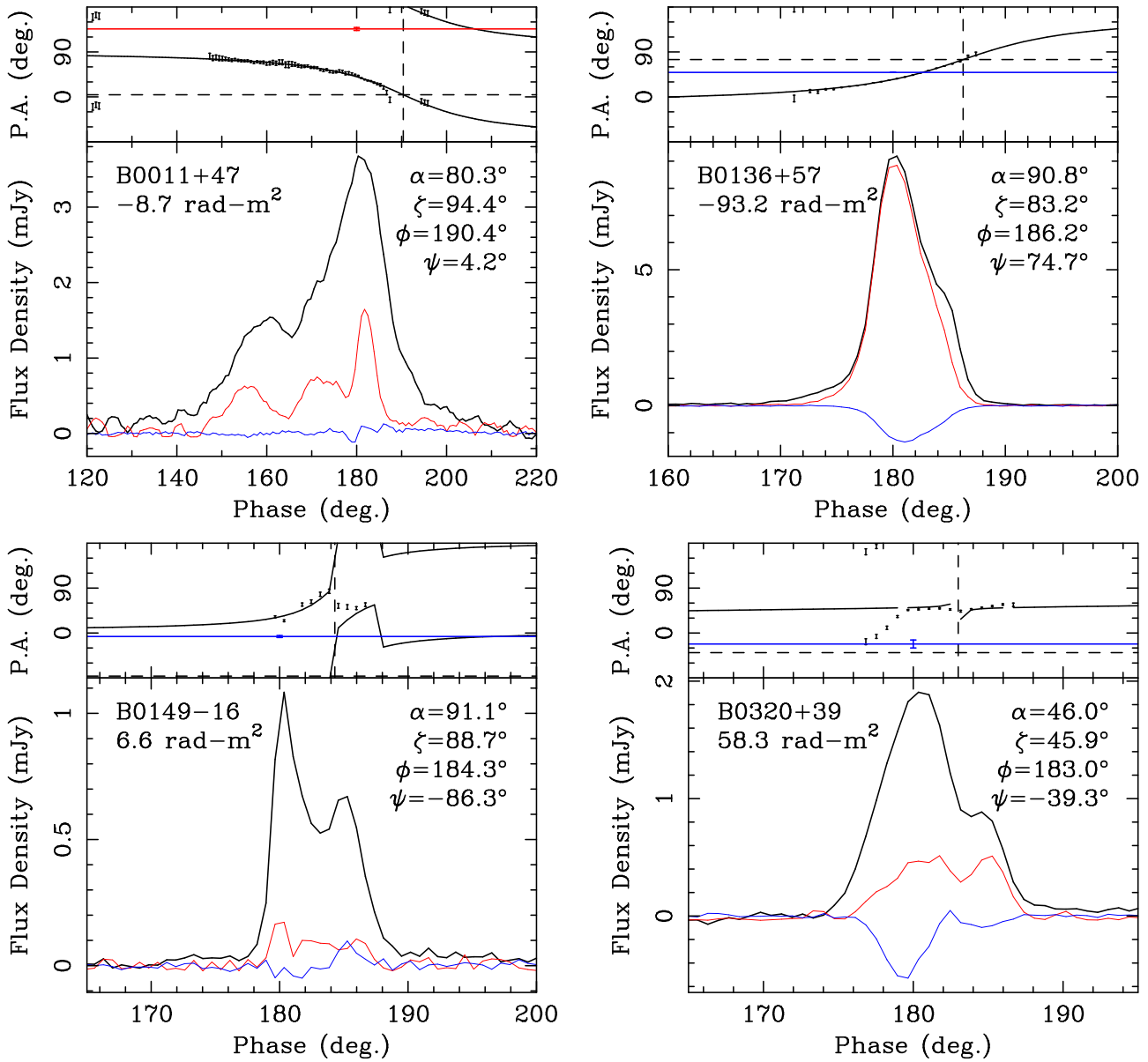


Figure A1. Polarization profiles and absolute PPA information for B0011+47, B0136+57, B0149-16 and B0320+39 as in Fig 1.

amenable to RVM fitting, and indeed the fit in Fig. A6 has little meaning in that we have fitted only the early linear PPA values and set the fiducial longitude at 180.5° . We thus have no recourse but to assume the fiducial longitude is aligned with the profile peak.

B1905+39 seems to provide a rare example of a conal quadruple cQ profile—that is an **M** with little or no core emission. ET VI provides a quantitative model for the star’s geometry which gives a secure foundation for the RVM fit in Fig. A6. and indeed the fiducial longitude falls very close to the profile center as expected.

B1911-04 is one of the best examples of a pulsar showing a core single **S_t** evolution—from a symmetrical Gaussian-shaped feature at meter wavelengths (GL) to three-lobed form, core and conal “outriders” at high frequency (vH). Unfortunately, the small fractional lin-

ear polarization makes the PPA traverse difficult to fit with an RVM curve. After correcting for the OPM offset on the profile’s leading edge, however, the fit in Fig. A6 appears to be reliable.

B1929+10 is perhaps the best polarization calibrator in the northern sky, and we were able to include it in our program as a diagnostic on two of the three days of observation. The polarized profile in Fig. 1 gives an RVM fit that appears reliable under the main pulse, but not so in the region of weak baseline polarization following the MP including the IP—and the second observation is very similar. For such a strong pulsar, weak RFI would not be discernible in this region but could distort the PPA traverse—and this appears to be what has happened. Other workers including Blaskiewicz *et al.* (1991) and Everett & Weisberg (2001) found that the main-pulse

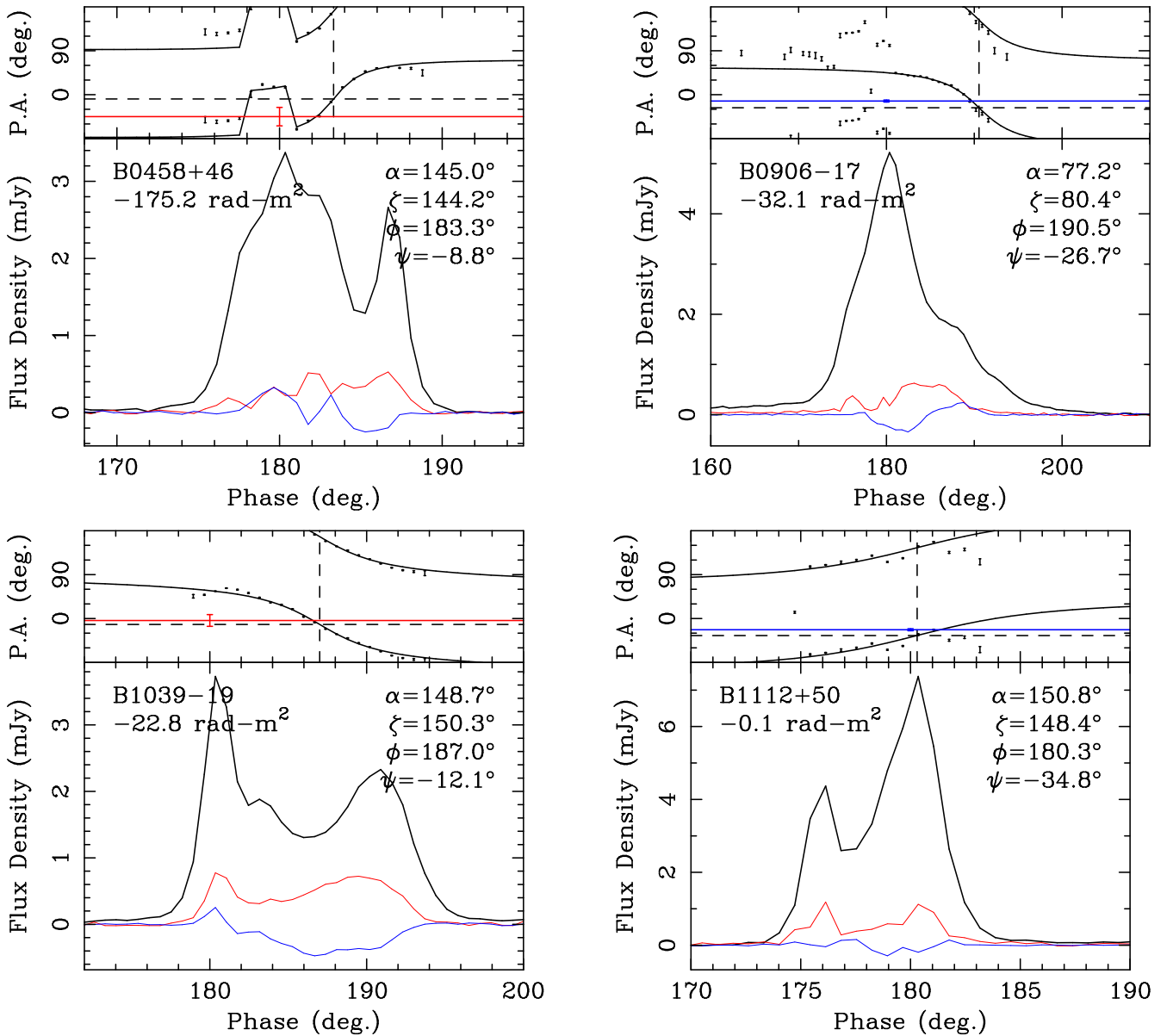


Figure A2. Polarization profiles and absolute PPA information for pulsars B0458+46, B0906-17, B1039-19 and B1112+50 as in Fig 1.

region had to be unweighted to achieve an acceptable RVM fit—and that the inflection point of such fits fall 15-20° earlier than the main-pulse peak. We rather unweighted much of the off-pulse region, and our inflection point falls close to this peak.

B2106+44: GL’s profiles together with our own in Figure A7 indicate a conal single \mathbf{S}_d or perhaps inner cone double \mathbf{D} profile, and WES/WSE do report a strong low frequency modulation feature in this star. The pulsar’s PPA traverse is very nearly linear, so an RVM fit is difficult and the resulting fiducial longitude not accurately well determined. Nonetheless, the fiducial longitude seems plausible.

B2111+46: This pulsar has a classic core-cone triple \mathbf{T} profile, the expected steep PPA traverse and substantial

fractional linear polarization across its entire profile. The geometric model in ET VI provides a foundation for the fit in Fig. A7, and the fiducial longitude falls near the center of the profile as expected.

B2148+63: The evidence seems strong per ET VI that this star’s profile is of the conal single \mathbf{S}_d . It broadens substantially at low frequency (GL, MIS) but scattering may also be a factor. This interpretation is strengthened by the drift modulation detected by WES/WSE. Fortunately, the significant linear polarization (see Fig. A7) does define the PPA traverse well, and the fiducial longitude is decently determined; it does fall late on the trailing side of the profile, but many such \mathbf{S}_d stars are asymmetric in just this manner.

B2154+40: Many published studies indicate that this

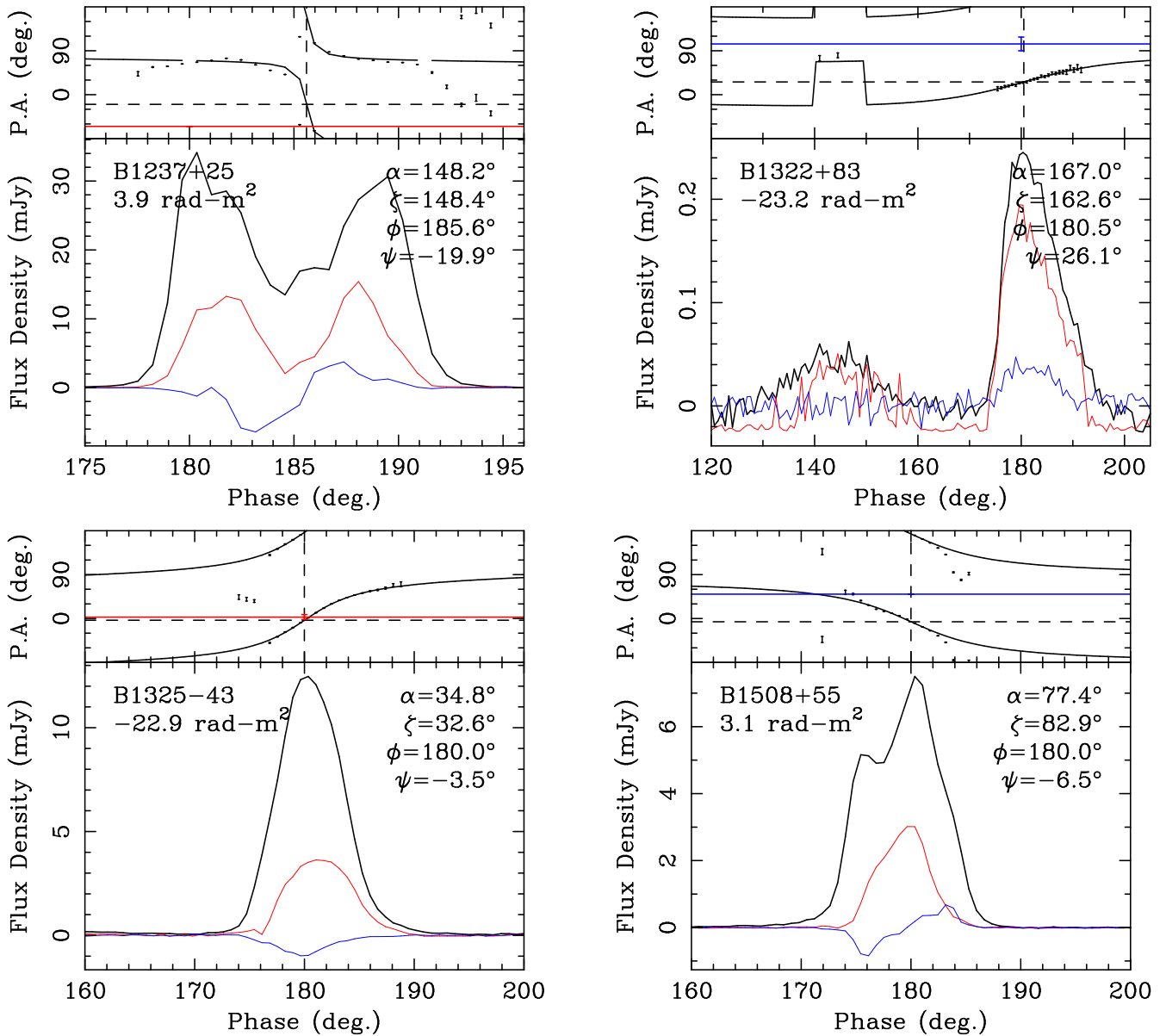


Figure A3. Polarization profiles and absolute PPA information for pulsars B1237+25, B1322+83, B1325-43 and B1508+55 as in Fig 1.

is a conal profile, either a narrow double **D** or conal triple **cT** as classed by ET VI. Moreover, WES/WSE confirm this interpretation by finding modulation features at both frequencies. The PPA traverse is strong and regular across many octaves [e.g., vH at 4.9 GHz and Suleymanova *et al.* (1988) at 102.5 MHz], therefore the RVM fit in Fig. A7 appears accurate and reliable.

B2217+47 appears to be a good example of a core-single **S_t** pulsar (GL), though only at the very highest frequencies do we see any hint of conal “outriders” (MGSBT). Some profiles show a PPA traverse rate of about $+8.5^\circ/^\circ$, and this provides a basis for the geometric model in ET VI. Apart from the edges the fit in Figure A8 appears reliable, and we see only a hint of the variable “postcursor” reported by Suleymanova & Shitov (1994).

B2224+65: This star has long been seen as having a conal double profile, but its two components are so dissimilar in form, spectrum and polarization as to render this interpretation virtually impossible. Again, vH gives the best comparative discussion using GL’s profiles. All the published polarimetry as well as ours in Fig. A8 show that the PPA under the trailing feature to be virtually flat; whereas at high frequency the leading one is so depolarized that no fit is possible. (The early low level linear polarization, including that under the leading feature, is surely corrupted by RFL.) In ET IX, we made a new GMRT observation of the pulsar at 325 MHz and interpreted the leading MP feature as having a core-single **S_t** profile and the trailing one as being a postcursor. We were able to fit an RVM curve to both the leading main

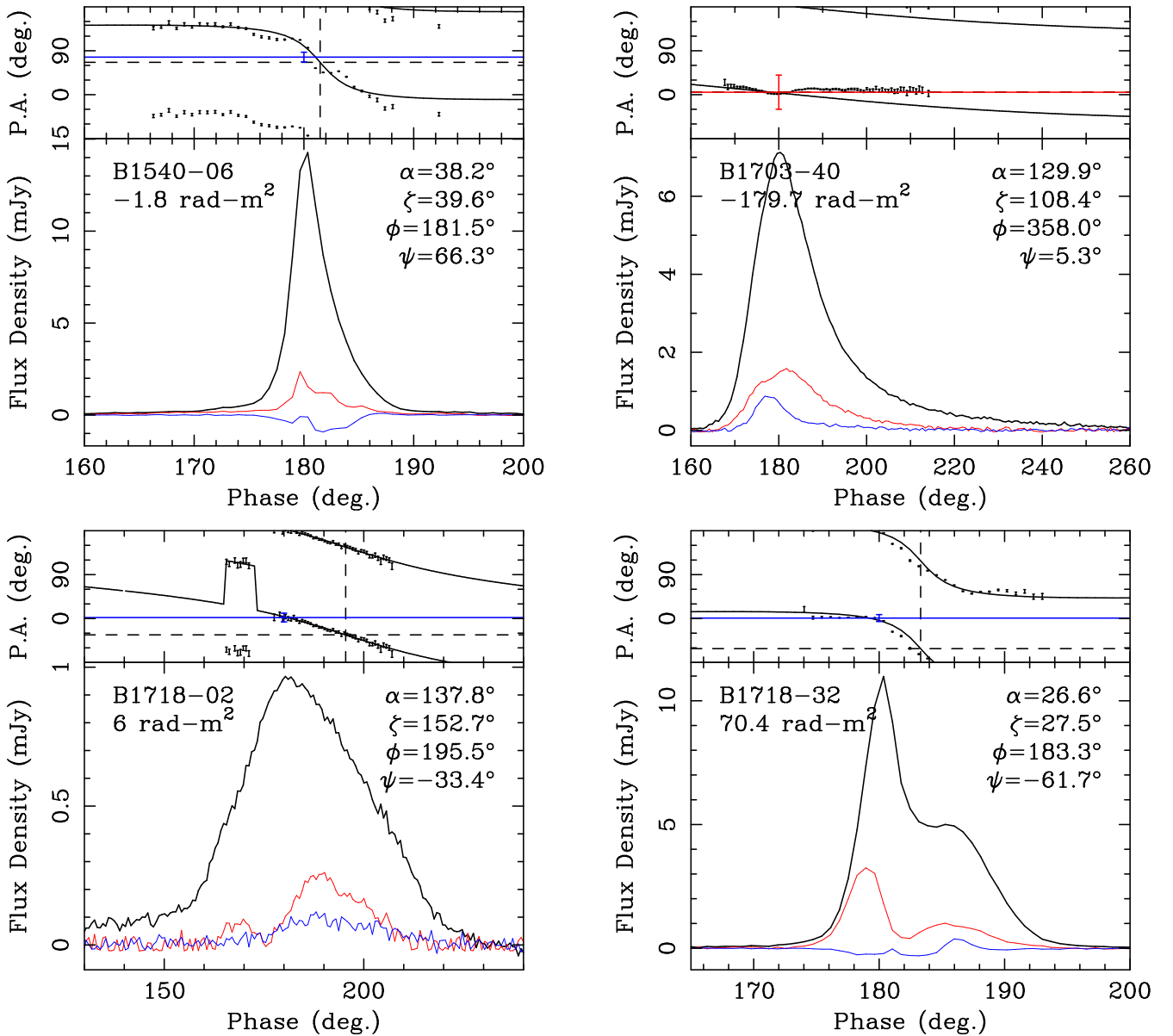


Figure A4. Polarization profiles and absolute PPA information for pulsars 1540-06, B1703-40, B1718-02 and B1718-32 as in Fig 1.

pulse and postcursor (see their fig. A10, upper right; α , $\beta = 166^\circ$, -3.8°). So, here we take the 325-MHz RVM fit as evidence that the fiducial longitude falls very close to the MP peak, and we compute the PPA at this point by extrapolating from the postcursor using the 325-MHz fit values.

B2255+58: This star was classified at having a \mathbf{S}_t profile in ET VI, and the higher quality three-lobed form in Fig. A8 seems to support this. While the fractional linear polarization is small to slight, the PPA traverse in our profile is similar to what is seen in GL’s in this band. We have little recourse but to try to understand the “wiggles” as OPM dominance switches, resolve them and then fit the “straightened” traverse. The resulting fit in the above figure then seems plausible, with a fidu-

cial longitude falling just after the center putative core component.

B2310+42 is an interesting example of a five-component \mathbf{M} profile according to ET VI. An number of profiles suggest triplicity, but weak outer conal features are also seen on the far wings of many profiles (*e.g.* XRSS)—and indeed inflections corresponding to the five features can be discerned in our profile in Fig. A8. This said, the PPA traverse is very difficult to interpret and almost certainly corrupted by low level polarized RFI. GL’s 21-cm. profile also shows a steep central traverse with OPM dominance shifts on the edges. It also shows baseline power far preceding the MP. Perhaps this fit is the best that can be achieved with our observation, the inflection point seems unreliable, even if determined with a small formal error.

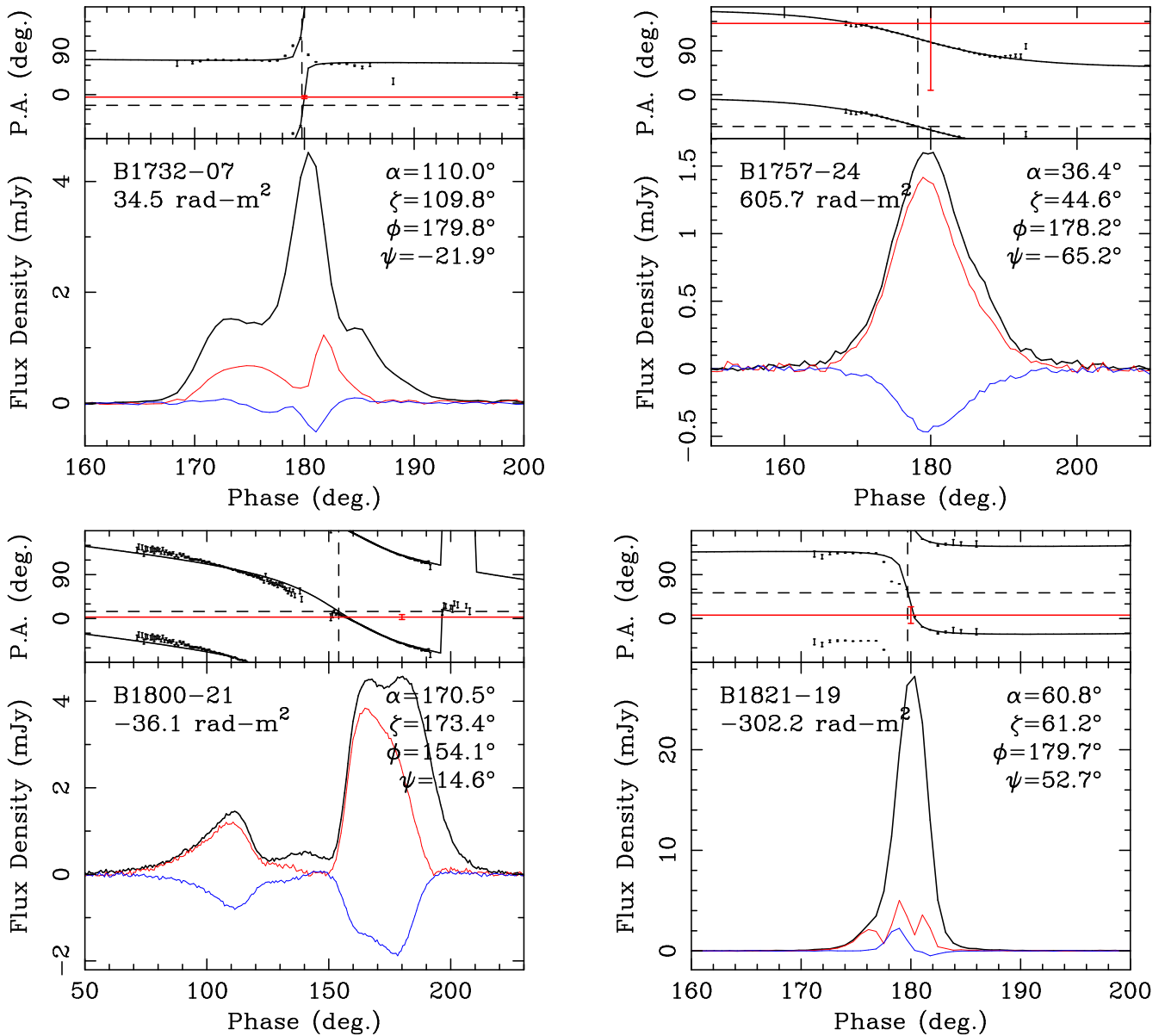


Figure A5. Polarization profiles and absolute PPA information for pulsars B1732-07, B1757-24, B1800-21 and B1821-19 as in Fig 1.

B2319+60 has a well studied conal triple cT profile per ET VI, and we see consistent properties over a band of at least four octaves (GL and vH). Moreover, WES/WSE identify the drift modulation feature and modes that were found in earlier work (Wright & Fowler 1981). The strong linear polarization and steep PPA traverse fix the fiducial longitude near the center of the profile as expected in Figure A9.

B2324+60: Not much is known about this pulsar beyond the older polarimetry of MGSBT, GL and vH—and that WES detect a strong drift feature. Interestingly, the better definition of the profile in Fig. A9 suggests that GL’s profile was not so well resolved. Still, without other polarimetry of similar quality across the band, it is very difficult to make a secure classification. Fortunately, said

seems unnecessary in this case as the PPA traverse is well defined and the RVM fitting results good and plausible.

B2327-20 has a triple T profile according to ET VI, based on polarimetry by MGSBT, GL and vH. The higher quality profiles measured by Johnston II confirm this interpretation. They also show how the large classic positive roughly 180° PPA swing at meter wavelengths become curtailed and distorted at higher frequencies as L/I decreases and profile narrowing conflates the polarization in adjacent regions of the profile. In this context, our profile in Fig. A9 seems to be decently measured, but even after correction for what seems to be the mid-profile OPM dominance shift, the RVM fit is poor.

B2351+61: Little study has been given to this pulsar. From the GL and vH profiles it is clear that it follows a

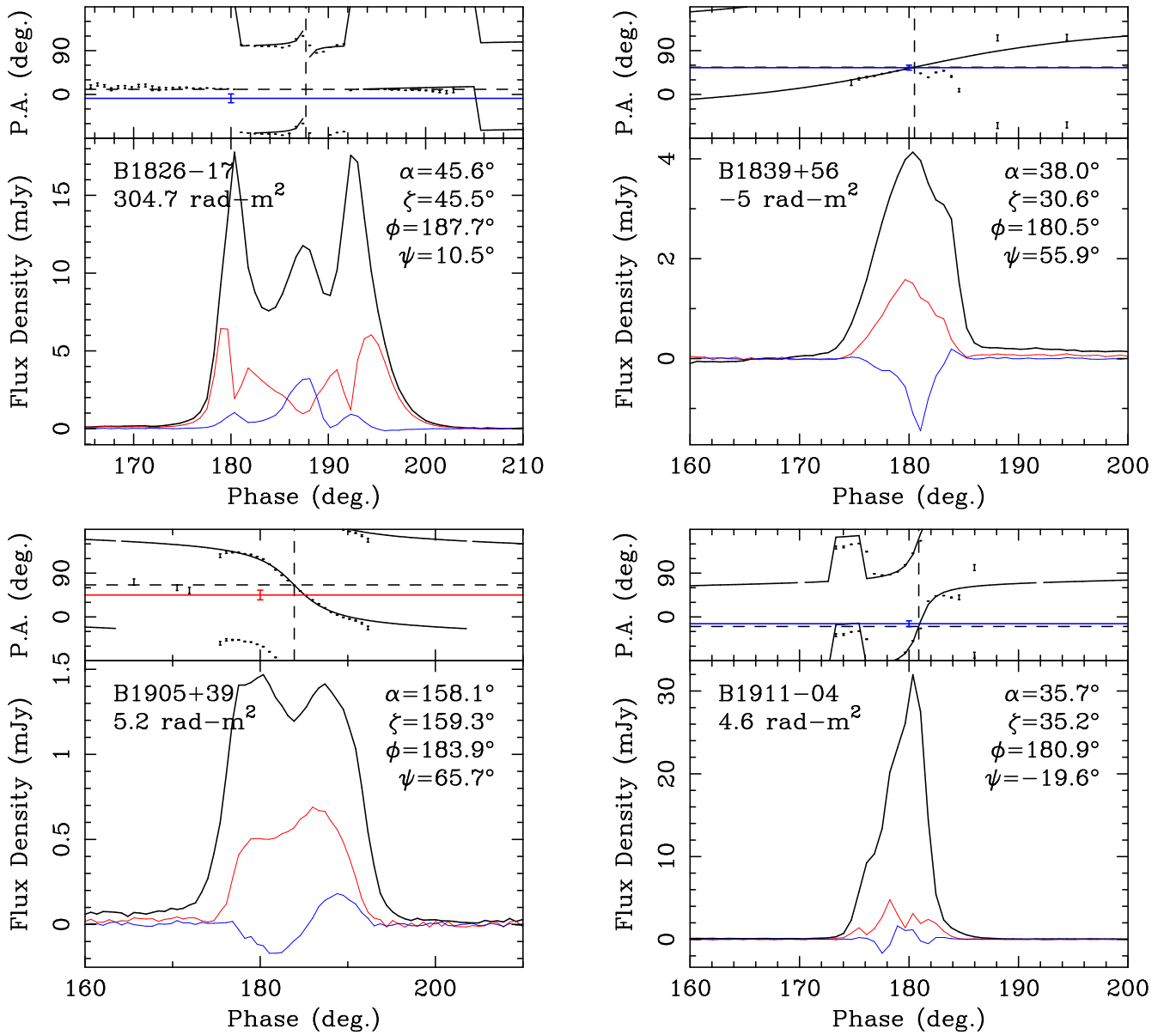


Figure A6. Polarization profiles and absolute PPA information for pulsars B1826-17, B1839+56, B1905+39 and B1911-04 as in Fig 1.

conal single \mathbf{S}_d evolution and indeed WES/WSE find evidence of drift modulation. The PPA traverse in Fig. A9 is orderly and regular apart from the usual OPM dominance shifts on the profile edges. The RVM fit seems reliable as the reduced χ_2 is very reasonable.

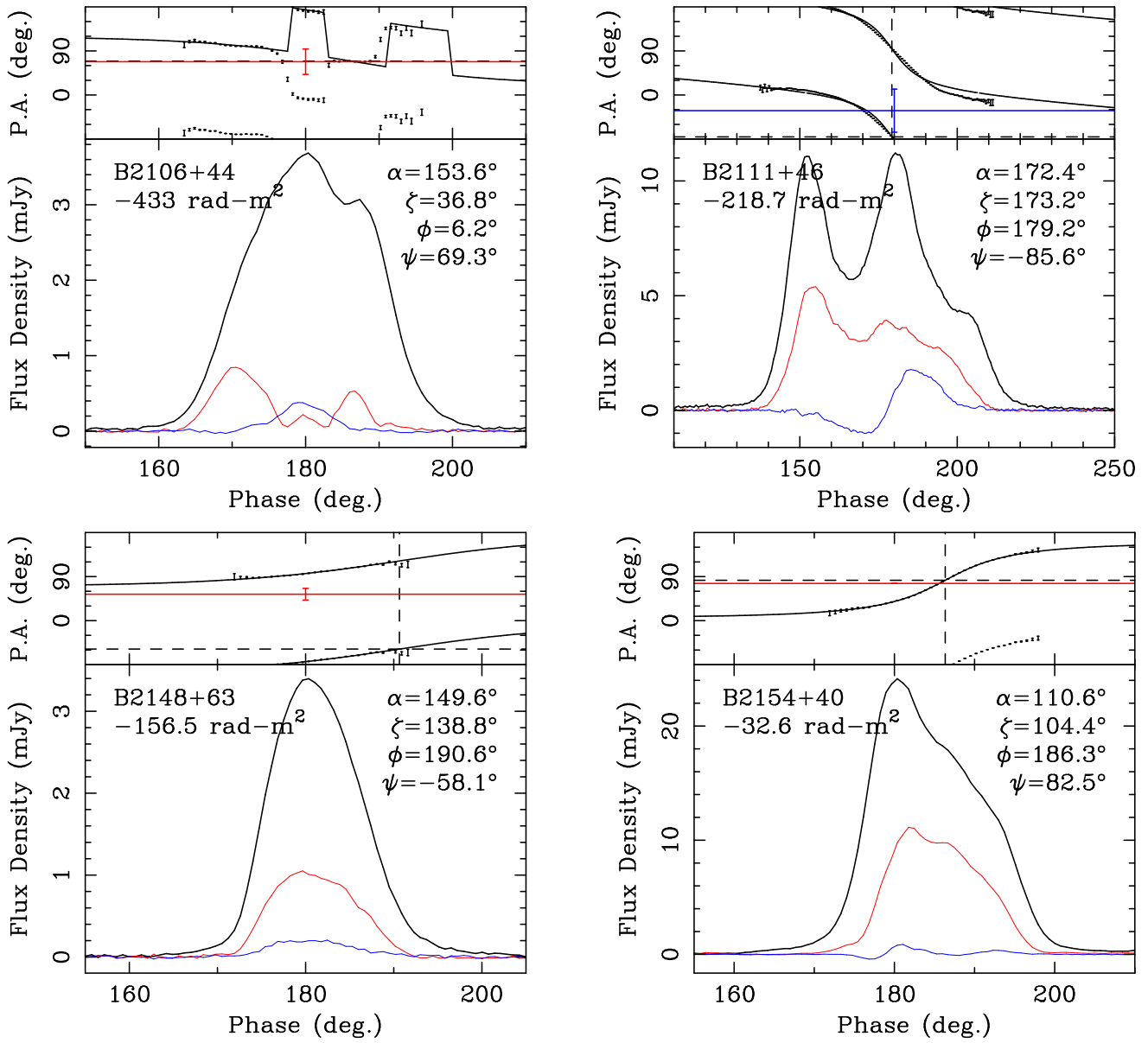


Figure A7. Polarization profiles and absolute PPA information for pulsars B2106+44, B2111+46, B2148+63 and B2154+40 as in Fig 1.

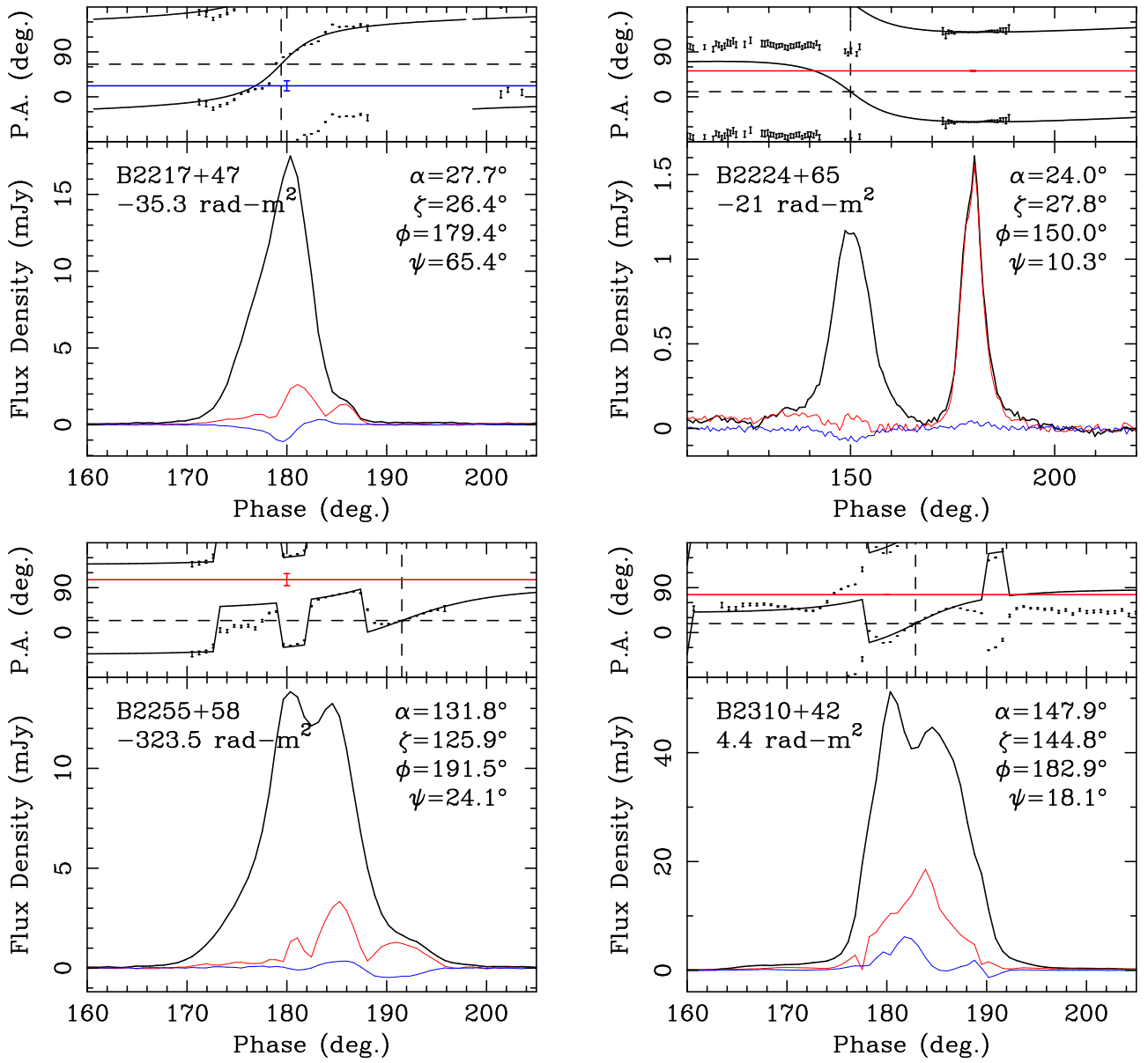


Figure A8. Polarization profiles and absolute PPA information for pulsars B2217+47, B2224+65, B2255+58 and B2310+42 as in Fig 1.

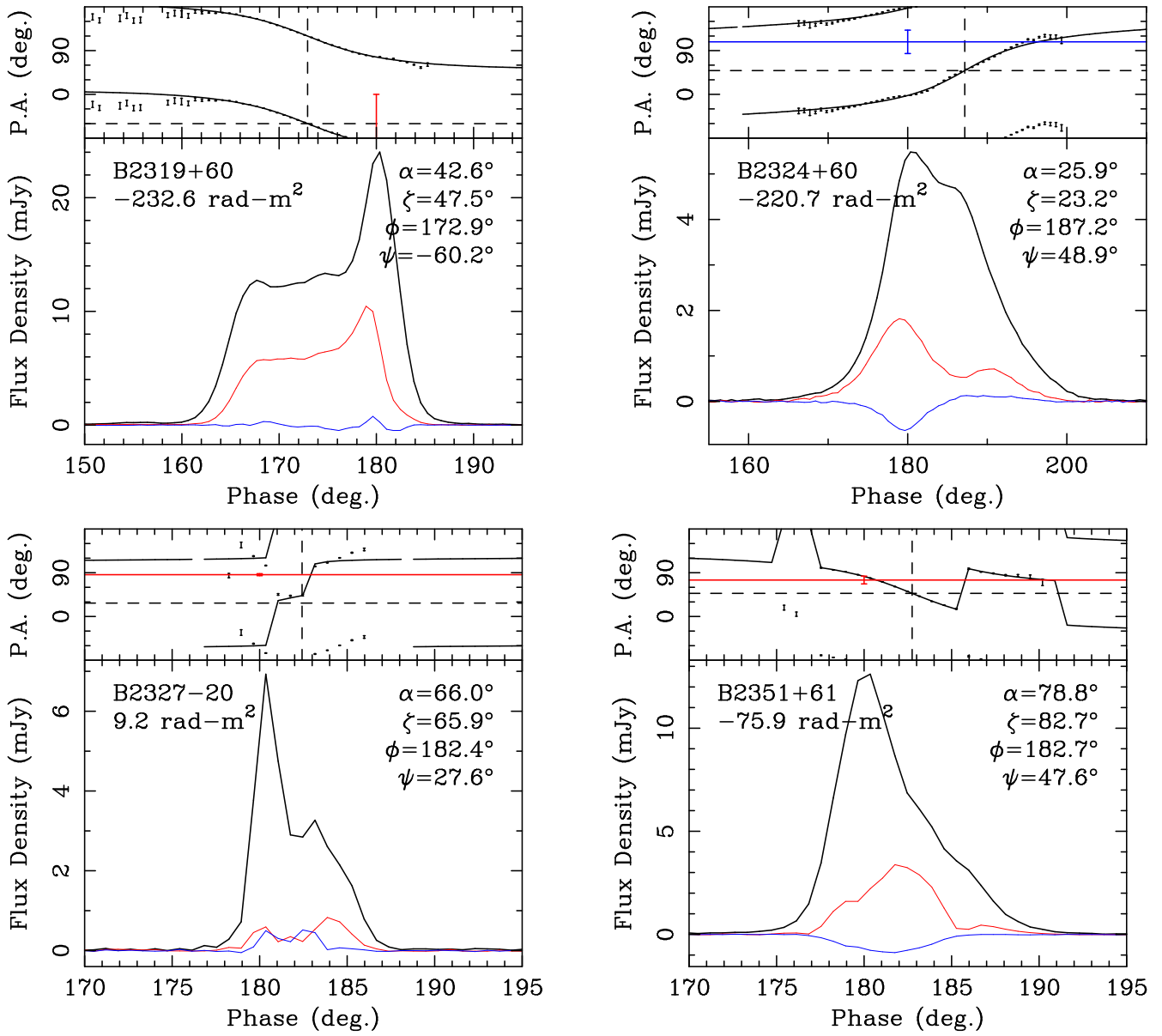


Figure A9. Polarization profiles and absolute PPA information for pulsars B2319+60, B2324+60, B2327-20 and B2351+61 as in Fig 1.